USAARL-TECH-FR--2026-37

UNITED STATES ARMY AEROMEDICAL RESEARCH LABORATORY

Development and Evaluation Methodologies to Statically Assess Restraint System Designs and Release Loads for Post-Crash Occupant Survivability

Michael B. Schlick, Lucia M. Melara, Danielle Rhodes,
Joseph F. Willett, Christopher J. Utter, Shannon M. McGovern,
& B. Joseph McEntire

Notice

Qualified Requesters

Qualified requesters may obtain copies from the Defense Technical Information Center (DTIC), Fort Belvoir, Virginia 22060. Orders will be expedited if placed through the librarian or other person designated to request documents from DTIC.

Change of Address

Organizations receiving reports from the U.S. Army Aeromedical Research Laboratory on automatic mailing lists should confirm correct address when corresponding about laboratory reports.

Disposition

Destroy this document when it is no longer needed. Do not return it to the originator.

Disclaimer

The views, opinions, and/or findings contained in this report are those of the author(s) and should not be construed as an official Department of the Army position, policy, or decision, unless so designated by other official documentation. Citation of trade names in this report does not constitute an official Department of the Army endorsement or approval of the use of such commercial items.

REPORT DOCUMENTATION PAGE	*Form Approved* *OMB No. 0704-0188*

1. REPORT DATE *(DD-MM-YYYY)*: 24-08-2026

2. REPORT TYPE: Final Report

3. DATES COVERED *(From - To)*: 10/1/2024- 9/30/2025

4. TITLE AND SUBTITLE
Development and Evaluation of Methodologies to Statically Assess Restraint System Designs and Release Loads for Post-Crash Occupant Survivability

5a. CONTRACT NUMBER

5b. GRANT NUMBER

5c. PROGRAM ELEMENT NUMBER

5d. PROJECT NUMBER
MO240112

5e. TASK NUMBER

5f. WORK UNIT NUMBER

6. AUTHOR(S)
Schlick, M. B.[1,2], Melara, L. M.[1,2], Rhodes, D.[1,2], Willett, J. F.[1,2], Utter, C. J.[1,2], McGovern, S. M.[1,2], & McEntire, B. J.[1]

7. PERFORMING ORGANIZATION NAME(S) AND ADDRESS(ES)
U.S. Army Aeromedical Research Laboratory
P.O. Box 620577
Fort Rucker, AL 36362

8. PERFORMING ORGANIZATION REPORT NUMBER
USAARL-TECH-FR--2026-37

9. SPONSORING/MONITORING AGENCY NAME(S) AND ADDRESS(ES)
U.S. Army Medical Research and Development Command
Military Operational Medicine Research Program
810 Schreider Street
Fort Detrick, MD 21702

10. SPONSOR/MONITOR'S ACRONYM(S)
USAMRDC

11. SPONSOR/MONITOR'S REPORT NUMBER(S)

12. DISTRIBUTION/AVAILABILITY STATEMENT
DISTRIBUTION STATEMENT A. Approved for public release: distribution is unlimited.

13. SUPPLEMENTARY NOTES
[1]U.S. Army Aeromedical Research Laboratory; [2]Chenega Services & Federal Solutions, LLC

14. ABSTRACT
U.S. Army aviators may be exposed to various potentially harmful in-flight or impact events during their missions. In mishap scenarios, the restraint system is designed to secure the occupant to the seat and minimize collisions with the cabin, preventing injuries by maintaining spinal alignment (Willett et al., 2022). Even with the introduction of the U.S. Army Aircraft Crash Survival Guide in 1989, the lower extremities, head, thorax, and spine remain the leading injured body regions in mishaps (Desjardins et al., 1989; Labun, 2014). The first objective of this research aimed to develop a methodology to statically assess occupant restraint systems under 1 G loading, where 1 G represents an acceleration of 32.174 feet per second squared (ft/s2) and evaluate the new method. A conventional five-point restraint system and a Parachute Restraint Harness Assembly-56 Personal (PCU-56\P) torso harness (TH) were used to restrain a test surrogate in a seat inversion wheel fixture for testing. The second aim of this research was the development and execution of a restraint system release assessment methodology.

15. SUBJECT TERMS
Occupant flail, static 1G loading, torso harness, 5-point restraints, seat restraint system, static testing

16. SECURITY CLASSIFICATION OF: a. REPORT	b. ABSTRACT	c. THIS PAGE	17. LIMITATION OF ABSTRACT	18. NUMBER OF PAGES	19a. NAME OF RESPONSIBLE PERSON
UNCLAS	UNCLAS	UNCLAS	SAR	37	Amanda Hayes, MS
					19b. TELEPHONE NUMBER *(Include area code)* 334-255-6067

REPORT DOCUMENTATION PAGE (SF298)
(Continuation Sheet)

14. Abstract (continued)

A conventional five-point restraint with a quick release (as described in MIL-S-58095A (AV) was used to evaluate the assessment.Both assessments identified a need to design occupant restraint systems to prevent lateral flail in rotary-wing mishaps. The increased risk of injury during lateral flail, indicated in the static 1 G loading, combined with the risk identified with the five-point release mechanism further emphasized the need for a lateral dynamic seat performance requirement to assess injury risk to the upper extremities, which may prevent egress.

Executive Summary

U.S. Army aviators may be exposed to various potentially harmful in-flight or impact events during their missions. The seat's restraint system is designed to secure the occupant to the seat during aggressive or turbulent flight conditions, reduce risk of occupant impact with surrounding structures by minimizing occupant flail, and maintain spinal alignment during vertical impacts (Willett et al., 2022). Even with the introduction of the U.S. Army Aircraft Crash Survival Design Guide in 1989, the lower extremities, head, thorax, and spine remain the leading injured body regions in mishaps (Desjardins et al., 1989; Labun, 2014).

The first aim of this research was to develop a method to assess occupant restraint system performance under static 1 G loading, where 1 G represents the acceleration of gravity (32.174 feet per second squared [ft/s^2]), and to evaluate the methodology. A conventional five-point (5-PT) restraint system and a Parachute Restraint Harness Assembly-56 Personal (PCU-56/P) torso harness (TH) were used to restrain a human surrogate in a seat inversion wheel fixture. Four measurement techniques—motion capturing, coordinate measuring, three-dimensional scanning, and still image tracking—were used by U.S. Army Aeromedical Laboratory (USAARL) researchers to develop the static restraint assessment method.

The second aim of this research was to develop a method to assess a restraint system's release while statically loaded under the surrogate's full weight. A conventional 5-PT restraint with a quick release, as described in MIL-S-58095A (AV), was used when developing this method. Researchers identified a potential hazard when the release mechanism was not rotated with enough speed to completely disengage all four belts, indicating that an occupant with an injured or otherwise hampered upper extremity might not be able to egress effectively under test conditions herein.

The developed methods were sufficient to assess two different restraint systems under static 1 G loading and egress efficacy of the conventional 5-PT restraint with quick release. The measurement systems used in the static restraint assessment demonstrated the ability to reliably acquire the surrogate's torso displacement. The static restraint system method developed could also be used to assess other restraint systems. Two possible initial risks were identified, an increased risk of lateral flail associated with the 5-PT restraint and TH and the potential inability of the user to release the 5-PT restraint effectively. The initial risk assessment indicates a need for dynamic lateral testing to inform on occupant safety.

This page is intentionally blank.

Acknowledgments

The authors would like to acknowledge specific integral team members who assisted with this research study. Thank you to Amanda Warren, Steven Arntzen, Allison Robinette, Shawn Booms, Matt Ballard, Mikala Fjerstad, and Mason Perkins for their technical support during data collection. Thank you to Marcy Conti-Traxler for her editorial review of this product.

Thank you to our Service Members, SFC Hai Nguyen, SGT Cole Wagner, SGT Richard Oldham, SPC Zaria Melvin, SSG Devon Henry, and SPC Roque Rodriguez for their hands-on support during data collection.

Thank you to our collaborator from the Naval Air Warfare Center Aircraft Division (NAWCAD), Glenn Paskoff, for lending us a Parachute Restraint Harness Assembly-56 Personal (PCU-56/P) TH.

This page is intentionally blank.

Table of Contents

List of Figures

Table of Contents (continued)

List of Figures (continued)

Page

List of Tables

Table of Contents (continued)

List of Tables (continued)

This page is intentionally blank.

Introduction

During U.S. Army rotorcraft aviation missions, aviators may experience numerous injurious scenarios, which may range from unanticipated and aggressive flight maneuvers and atmospheric turbulence buffeting to hard landings and crashes. Sudden aircraft accelerative changes can cause the aircraft occupants to displace from their initial positions; therefore, restraint systems play a vital role in keeping aviators safe. During impact conditions such as hard landings and crash events, an effective restraint system will minimize upper torso and head flail (Willett et al., 2022) and prevent pelvic submarining (i.e., slipping under the lap belt) to mitigate injury risk and maximize occupant safety. Since the restraint system is integrated in the cockpit seats, the performance requirements of the restraints are embedded in the seat performance specification, MIL-S-58095A (Aviation [AV]) (Department of Defense [DoD], 1986). The MIL-S-58095A (AV) specifies a restraint release requirement of 50 pounds (lb) for a conventional rotary buckle restraint system, ensuring egress is possible when the occupant is fully inverted (upside down).

Past research addressed U.S. Army, Navy, and Air Force mishap kinematics, identifying the causes and rates of Class A, B, and C mishaps (Baker & Bellenkes, 1996; De Lorenzo et al., 1999; Knapp & Johnson, 1996; Shanahan & Shanahan, 1989). A retrospective review, comparing mishap data from 1970 through 1977 with previously published data, demonstrated that 33% of accidents classified as survivable had one or more fatalities (Sand, 1978). Moreover, this study showed that the extremities, head, and spine remained the “leading body areas to be injured” and that head injuries were more prevalent in mishaps where the aircraft rolled over (Sand, 1978, pp. 54-1). Crashworthiness improved with the advancement of technology and the introduction in 1989 of the U.S. Army Aircraft Crash Survival Design Guide (ACSDG), where *Volume Four* focuses on seat design, occupant restraint, and occupant survivability (Desjardins et al., 1989). A review of U.S. Army aviator injuries sustained in mishap events demonstrated that the most common injury causation was “secondary impact,” resulting from occupants flailing into structures (Shanahan & Shanahan, 1989, pp. 415). Another review of rotorcraft mishaps from mid-1977 to 2009 demonstrated that the head and extremities continued to be heavily affected by impacts regardless of aircraft type (Labun, 2014).

There are two primary styles of seating restraint systems in military aviation, a conventional n-point restraint system and a torso harness (TH) system. One, a conventional *n*-point restraint system (where *n* is the number of restraint attachment points to the seat), typically used for non-ejection seat aircraft, where the restraint system is attached to the seat and the occupant ‘buckles’ themselves into a seat using the restraint system. The TH system is typically used in ejection seat aircraft where it doubles as the parachute harness. The occupant wears the TH restraint system, and the system is ‘buckled’ into the seat (Willett et al., 2022). A prior report comparing the effectiveness of these two types of restraint systems determined that TH do not restrain the occupant as well as conventional seat restraints (Hearon et al., 1983). With innovative seating restraint system design concepts emerging, independent vetting is crucial in understanding the performance of such designs (e.g., flail reduction or injury hazard potential) as well as their use, risks, benefits, and compatibility with existing seating systems—for protecting rotorcraft aviation occupants.

The U.S. Army is considering a new pilot seating system as a potential replacement seat for the AH-64, UH-60, and new rotorcraft designs. New concepts for the occupant restraint systems include a TH and a dual 3-point (D3P) restraint, neither of which have been third-party tested. The purpose of this project was to develop the methods needed to assess and quantify the efficacy of two existing restraint systems and their release mechanisms, where applicable, in various seat orientations using the inversion wheel at the U.S. Army Aeromedical Research Laboratory (USAARL). These methods will provide a means to collect seated occupant flail displacement data, although the 1 G flail measures are not the same as the flail observed in dynamic loadings. These methods are not intended to be a replacement for dynamic testing, but to serve as a screening tool to eliminate restraint designs that perform poorly from further consideration and expense. Additionally, these methods will provide a means to measure the required effort to activate the restraint system release while under load. The ability to evaluate restraint systems in an operationally relevant mishap position enables USAARL to provide pertinent information to stakeholders to support decision-making for future seat restraint system designs.

Methods

This study was designed to establish two methods: (1) to assess the efficacy of restraint systems to hold a seated occupant in place; and (2) to assess the ease of releasing the restraint system at a pre-determined orientation. For the first methodology, a manikin underwent 1 G static loading during various pitches and rolls, where 1 G represents gravitational acceleration of 32.174 feet per second squared (ft/s^2). These test scenarios were meant to replicate operationally relevant mishap final positions. The USAARL inversion wheel is a manually operated, open-frame cylindrical structure supported by four rollers mounted on a base frame (Figure 1A). The frame was also supported on wheels to facilitate relocating the entire structure as needed. The open-frame cylindrical structure includes a rigid seat assembly mounted within the structure (Figure 1B). The seat assembly has a fixed 95-degree (°) bucket angle and was designed to accommodate a variety of aircraft restraint systems (Figure 1B). Additionally, the seat assembly can be mounted in two configurations allowing rotation along the seat's roll or pitch axis (Figure 2). The inversion wheel can be rotated 360° and secured in any rotational orientation with safety chains and/or ratchet straps. The starting position (0°) of the inversion wheel was defined as when the seat back was in the upright, vertical position and rotations were measured from this 0° starting position. The test occupant, an anthropomorphic test device (ATD), was restrained with the inversion wheel positioned in a neutral starting position (Figure 2).

This space is intentionally blank.

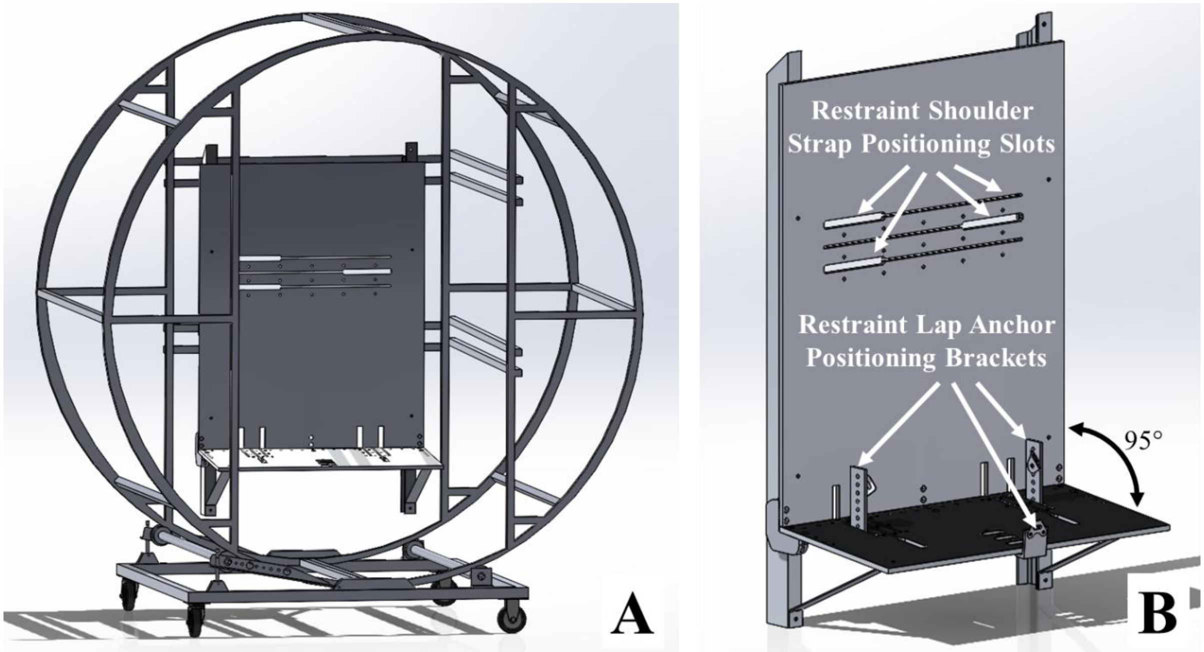

Figure 1. The USAARL inversion wheel is an open-frame cylindrical structure resting on rollers of a wheeled frame (A). The inversion wheel has a seat assembly (roll setup pictured [A]) designed to accommodate the restraint systems of multiple platforms (B).

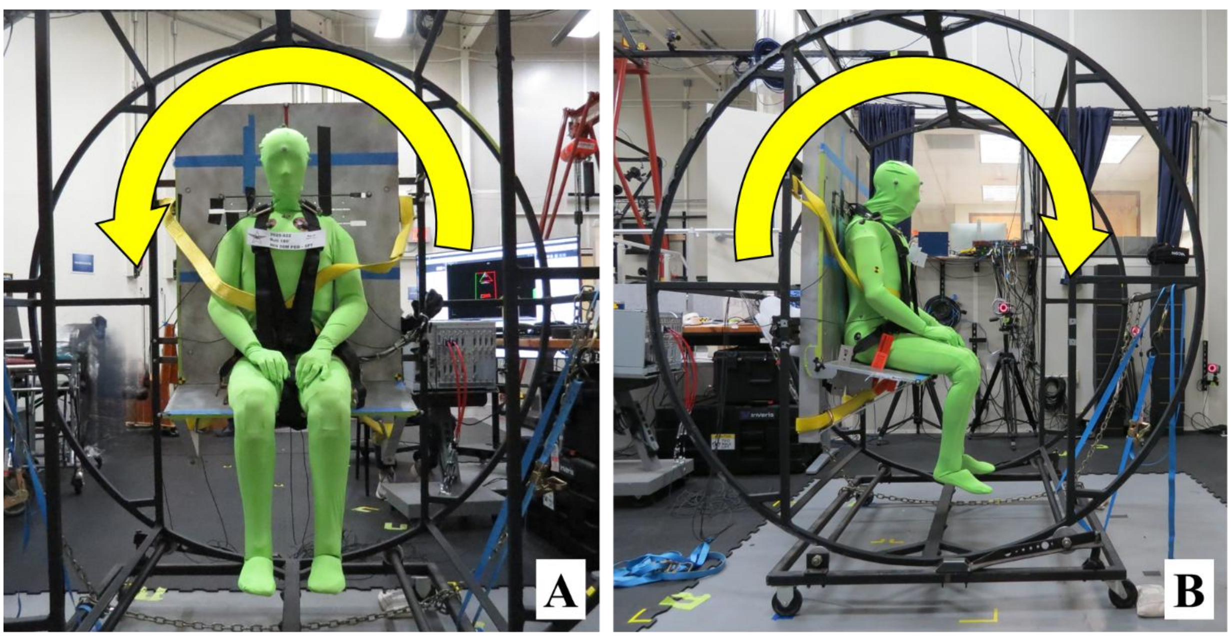

Figure 2. The test seat assembly can be mounted to allow rotation along the roll (A) or pitch (B) axis. The ATD and the 5-point restraint system is pictured in the neutral position. The yellow arrows indicate the direction of right roll (A) and forward pitch (B). Blue ratchet straps were used to hold the wheel in the 0° position.

Development of the Static Restraint System Assessment

The static restraint assessment method was developed to measure the occupant flail, as measured by chest displacement. Two ATDs were assessed and four measurement techniques (motion capture, coordinate measuring machine, three-dimensional [3D] scanning, and image tracking) were evaluated.

ATD selection.

Two similar ATD designs were identified for potential use in the restraint assessment methodologies. The ATD design difference was their pelvic design (seated versus articulating) which were assessed for compatibility with the seat assembly. The ATD pelvis and restraint interaction were inspected during inversion wheel rotation to ensure the restraints did not get caught in the gaps or creases of the ATD joints. The Federal Aviation Administration (FAA) Hybrid III (HIII) 50th percentile male (50M) ATD (The Humanetics Group, Farmington Hills, MI) was used as the seated pelvis model. The seated pelvis is molded in a 90° angle with a straight spine. The HIII-50M Pedestrian (P) (The Humanetics Group, Farmington Hills, MI) was used with an installed pedestrian kit (JASTI Co., LTD, Tokyo, Japan) as the articulating pelvis model. The articulating pelvis has a sit-to-stand construction with a straight spine.

The FAA-HIII-50M with the molded seated pelvis was difficult to position into the seat. When seated naturally, the shoulders were displaced from the seat back surface. When securing this ATD with the restraint system, the upper torso was pushed aftward against the seat back surface, introducing an extension motion of the lumbar spine, requiring the straight lumbar spine to be torqued to position for the torso of the ATD to rest against the seatback (Figure 3). As a result, a gap was formed between the seatback and the lower torso, indicated by the blue line in Figure 3A. In contrast, the HIII-50M-P pelvis was easier to position since the hips articulate more freely than the molded seated pelvis (Figure 3B). It was also hypothesized that the lower extremity of the HIII-50M-P would flail more realistically with the added articulation provided by its pelvis design; therefore, the HIII-50M-P was selected to develop the static restraint assessment methodology.

This space is intentionally blank.

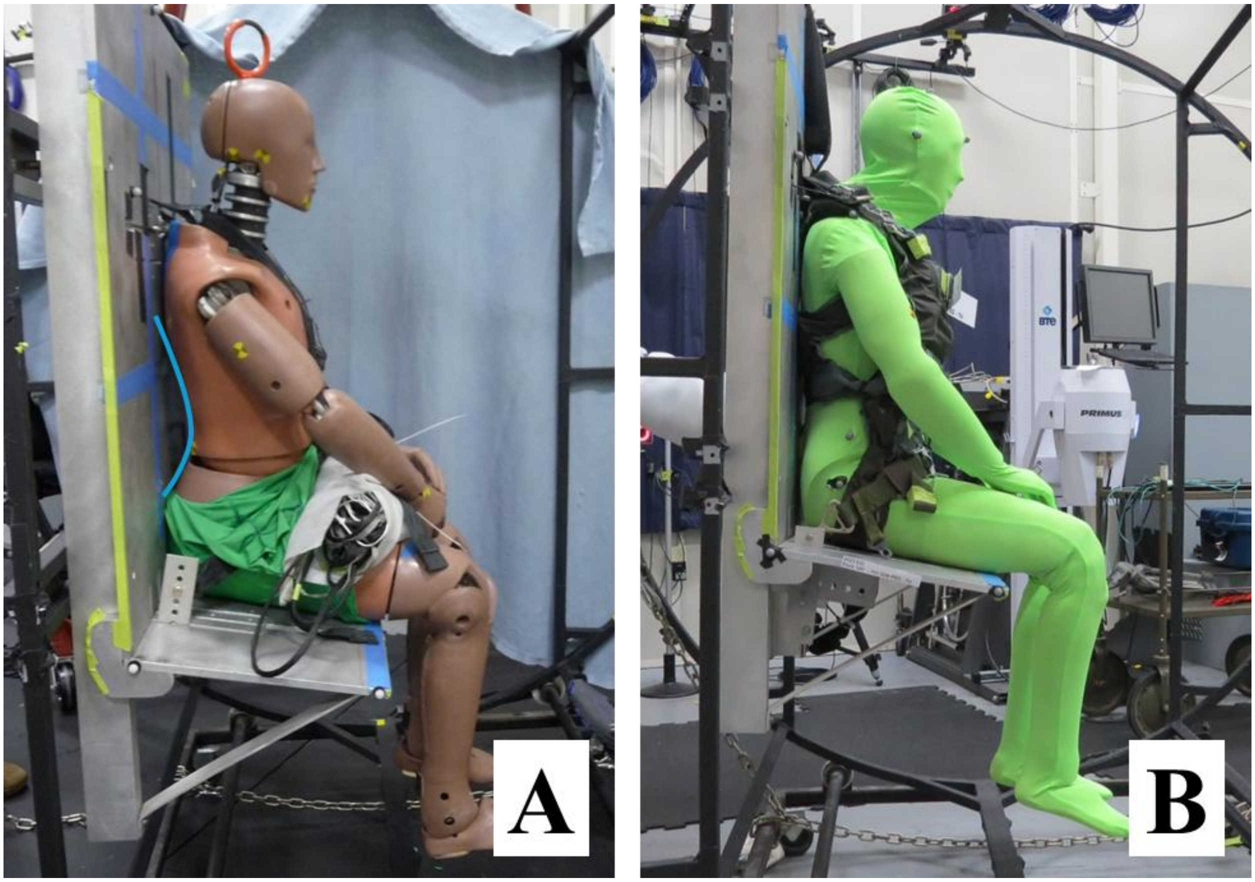

Figure 3. The FAA-HIII-50M (A) and HIII-50M-P (B) were tested to determine their compatibility with the seat assembly. The molded pelvis of the FAA-HIII-50M made positioning difficult and left a gap between the seatback and the ATD back (indicated by the blue line [A]). The articulating pelvis of the HIII-50M-P allowed for better positioning of an occupant with most of the back in contact with the seatback.

This space is intentionally blank.

ATD setup and positioning.

The HIII-50M-P adjustable joints were set at, or looser than, the “1 G” setting specified in the user manual (Humanetics Innovative Solutions Inc., 2017) to simulate a relaxed occupant rather than a braced occupant. Spherical, retroreflective fiducial markers were affixed to the ATD flesh with double-sided adhesive tape before fitting the ATD with a lightweight, stretchable body suit (a “green screen suit”). To ensure marker visibility, the suit was slit at each marker. The ATD was then fitted with a Parachute Restraint Harness Assembly-56 Personal (PCU-56/P) size large (TH) on loan from the Naval Air Warfare Center Aircraft Division (NAWCAD). The excess length of the harness strap ends were folded and wrapped to not interfere with the visualization (Figure 4A, red squares). Although the ATD was instrumented, the sensors were not used for this study, and the instrumentation cables were routed through the back of the harness to not interfere with the test (Figure 4B).

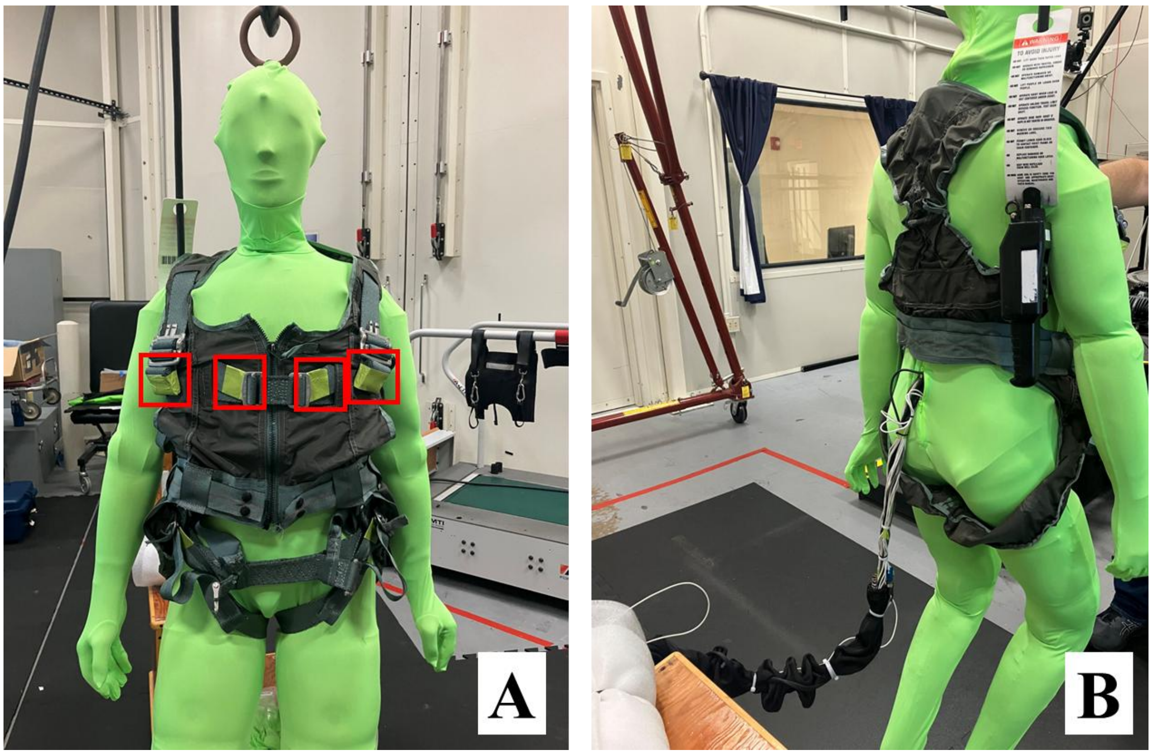

Figure 4. The HIII-50M-P was fitted with a PCU-56/P size large TH with the excess of the harness straps folded and wrapped (red squares) (A) and the instrumentation cables routed through the back of the harness (B).

The inversion wheel was positioned and secured in the 0° starting position with ratchet straps. The ATD, wearing the TH, was placed into the seat of the inversion wheel and the TH was fastened to the anchors on the seat assembly (Figure 5A). The instrumentation cables were routed, stowed, and secured for testing (Figure 5B). The shoulder restraint straps, which were instrumented with belt load cells (Model 5K-CL-X5K-2, Humanetics Innovative Solutions, Farmington Hills, MI), were adjusted to provide a webbing tensile force between 5 and 10 pounds (lb) (Figure 6). Belt load cell data were collected at 250 samples/second (s) with a Synergy data acquisition system (Hi-Techniques, Inc., Madison, WI).

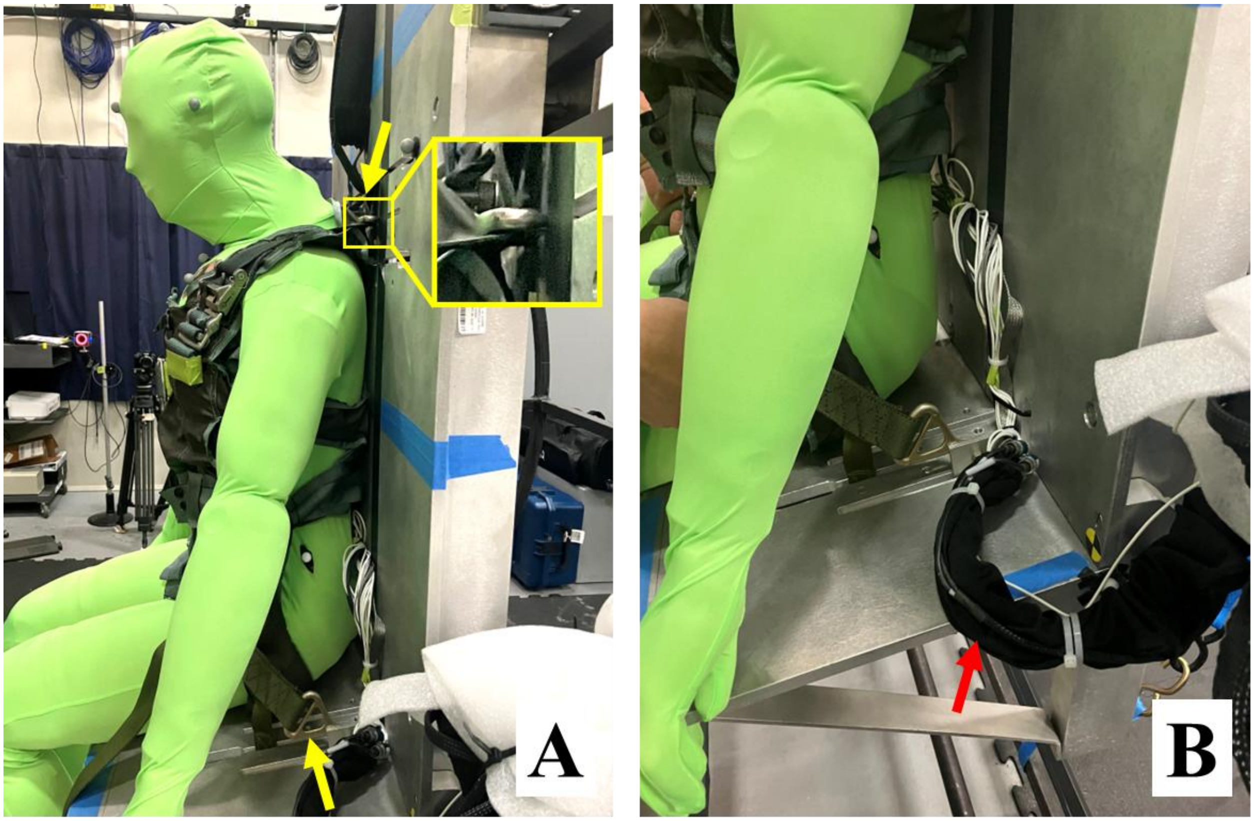

Figure 5. The ATD was secured to the seat assembly via the PCU-56/P TH anchors (yellow arrows) (A). A close-up photo of the shoulder anchors is shown in the yellow square. The instrumentation cables (red arrow) were routed and secured out of the way (B).

This space is intentionally blank.

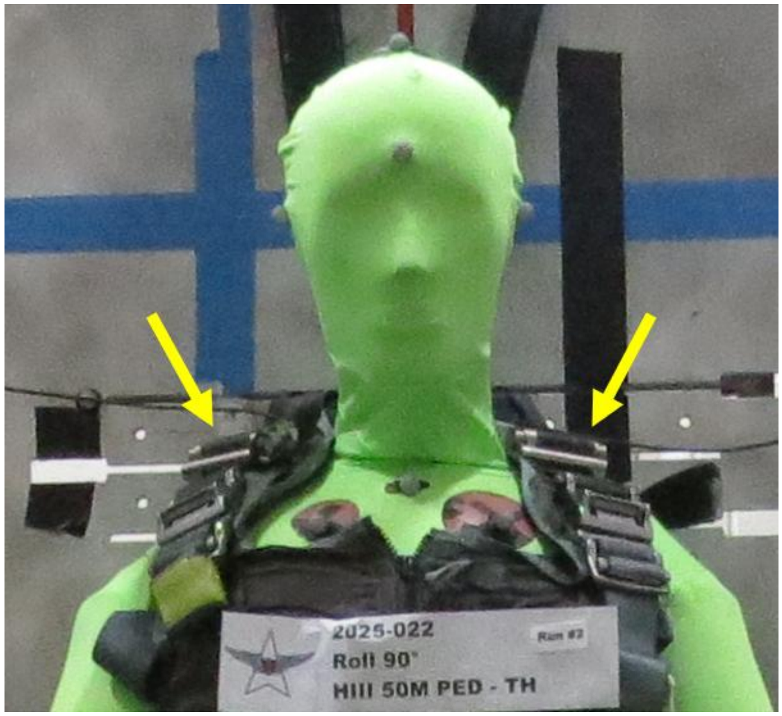

Figure 6. The TH straps were instrumented with load cells (yellow arrows), where possible.

Next, the ATD was positioned in a neutral, seated posture (Figure 2) for the pre-test measurement. The hips were positioned so that the upper legs and back followed the 95° bucket angle of the seat assembly with the back of the pelvis touching the seatback. The upper arms were positioned against the sides of the chest with the elbows forward of the mid-coronal plane, about even with the front of the chest. The hands were placed palms down at about mid-thigh. The upper legs were neutral, neither abducted nor adducted, the lower legs hung parallel to each other, and the knees and ankles were flexed to about 90°.

This space is intentionally blank.

Measurement techniques.

Four measurement techniques (motion capture, coordinate measuring machine, 3D scanning, and image tracking) were evaluated to measure the ATD chest displacement between the fixture 0° position and the 90° pitch and 90° roll positions. The following equipment systems were selected to collect data during the study:

- A Vicon motion capture system (Nexus Version 2.6, Vicon Motion Systems, Oxford, UK) was used to capture data throughout the inversion wheel rotation.
- A Quantum Max FaroArm® coordinate measurement machine (CMM) (FARO Technologies, Lake Mary, FL) was used to measure the pre- and post-rotation data.
- An Artec Leo 3D Scanner (Artec 3D, Senningerberg, Luxembourg) was used to scan the pre- and post-rotation positions of the ATD and seat.
- Photographs documenting the pre- and post- positions of the ATD were taken for two-dimensional (2D) image tracking in TEMA Pro 2D (Image Systems, Phoenix, AZ).

Spherical, 12 millimeter (mm), retroreflective markers were used as fiducials for every measurement system for positional coordinates. The markers were placed on ATD landmarks to measure occupant excursion from the seat (Figure 7). Four markers were attached to the ATD head coincident to the head center of gravity: one on the right, left, top, and front. Five markers were attached to the torso: two approximating the left and right acromion processes, one approximating the upper sternum, and one each about 2 inches (in.) left and right laterally from the mid-sternum approximation. Two markers were attached to the pelvis at the superior-inferior midpoint: one on the right and one on the left. Two markers were attached coincident to the femoral heads (“H-Point”): one on the right and one on the left (Figure 7). Three markers were attached to the outside edges of the seatback: one at the upper right, one at the upper left, one at the top midpoint. Four markers were attached to the outside edges of the seat pan: two each at its front edges, one on the right and one on its left, and two each at its back edges (Figure 8).

This space is intentionally blank.

Figure 7. Retroreflective markers were placed on the ATD to capture displacement during the rotation of the inversion wheel.

This space is intentionally blank.

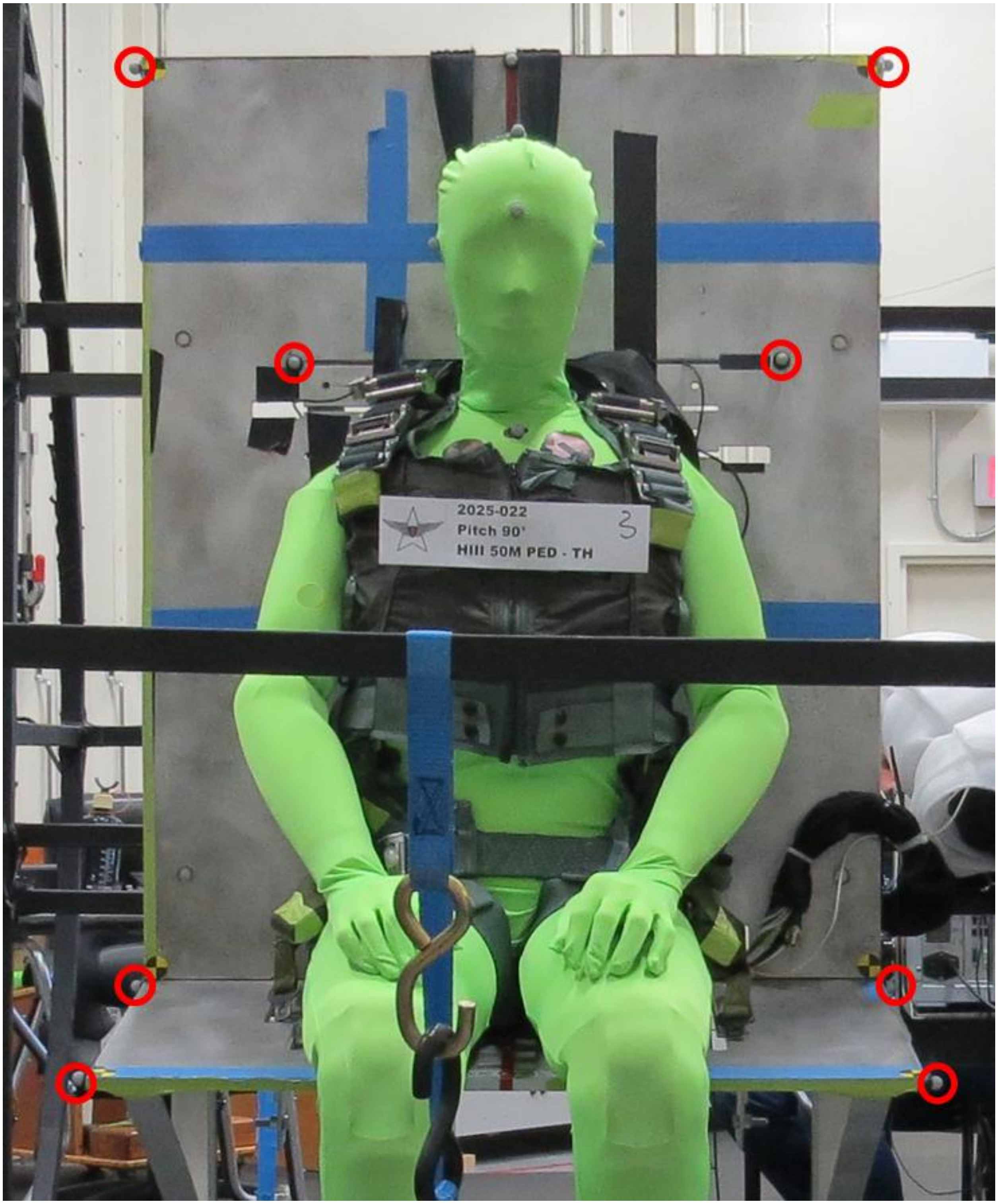

Figure 8. Retroreflective markers (red circle) were placed on the seatback and seat pan for the reference from which to measure occupant displacement.

Coordinate axes.

The plane of the seatback was selected as the reference axes system in which to measure occupant displacements, where the +*x*-axis was forward, +*y*-axis was leftward, and +*z*-axis was upward. Specifically, the +*y*-axis was defined as from the lower right seatback marker to the lower left seatback marker. A temporary +*z*-axis was defined as from the lower right seatback marker to the upper right seatback marker. The +*x*-axis was defined as the cross product of the +*y*-axis and temporary +*z*-axis, and, to ensure +*z*-axis orthogonality, the final +*z*-axis was defined as the cross product of the +*x*-axis and +*y*-axis. As the chair was rotated, the axes remained fixed with respect to the seatback.

Vicon motion capture system.

A Vicon motion capture system of 20 cameras (8 model Bonita, 2 model Vantage, and 10 model Vero) was used to record 3D coordinates, where cameras were distributed overhead, in front, and to the left and right of the upright seated occupant, resulting in a capture volume of about 20 feet wide by 10 feet deep by 10 feet high. Each camera was aimed at, zoomed, and focused for the anticipated range of motion of the occupant. The cameras were "calibrated" (their locations and orientations were calculated by the Vicon system) via a typical wand of five known markers waved throughout the capture volume. Using the Vicon Nexus software, each rotation event was recorded at 240 frames per second from about 1 second before the event start time to about 5 seconds post-event, then the data were processed and exported.

MATLAB (MathWorks, Inc., Natick, MA) was used to develop the code to import the 3D coordinates of each marker, transform the coordinates from the Vicon axes to the seatback reference axes, and export the transformed data. The lower right seatback marker was used as the origin. The occupant displacement was reported using the upper sternum marker with respect to the seatback as the chair moved.

FARO Quantum Max FaroArm® CMM.

The FARO Quantum Max FaroArm® CMM was placed on its portable tripod base to measure the pre- and post-rotation locations of the spherical markers on the ATD and the inversion wheel seat. A user-defined coordinate system was created, and all retroreflective marker locations were captured with respect to that coordinate system. The lower right-hand seatback sphere was used as the origin (0,0,0). Using the CAM2 software, spherical marker measurements were collected before and after the rotation event. Marker location coordinates were exported to text files and analyzed in MATLAB or Microsoft Excel. The post-processing axes transformation method used for Vicon was also used on the FARO data to align coordinate systems between the measurement systems.

This space is intentionally blank.

Artec Leo 3D scanner.

The ATD and seat were scanned pre- and post-rotation with a handheld Artec Leo 3D scanner. Scans were conducted until the ATD and seat assembly were sufficiently acquired. If there were gaps in the scan, the user rescanned that part of the ATD and/or seat assembly. The scans were imported into SolidWorks, from which the spherical markers' coordinates were obtained. The post-processing axes transformation method used for Vicon was also applied to these data.

Image tracking (TEMA).

Still images were taken from the front of the ATD to capture the roll rotations and from the right side of the ATD to capture the pitch rotations to record the ATD excursion from the seat. Pre- and post-rotation images were taken on two Canon PowerShot SX50 high sensitivity cameras (Canon USA, Inc., Melville, NY) set perpendicular to the inversion wheel seatback and focused on the ATD torso. Distance measurements were taken from the camera lens to a reference point and the cameras remained in their locations for each test configuration. The pre- and post- still photos were processed into a video format via MATLAB. The spherical markers were tracked using TEMA to measure the marker coordinates and evaluate occupant 2D excursion from the seat. The TEMA data were scaled using known dimensions: in roll, the width of the seatback along the top edge; and in pitch, the width of the lap belt anchor. The axes definitions and polarities used for Vicon and FARO were matched in TEMA.

Measurement systems acquisition methodology.

The inversion wheel was rotated to a 90° forward pitch. Each rotated position was repeated three times to validate the data, ensure reliability of the data, and check the experimental design. Belt load cell and Vicon data were captured pre-, post-, and during the rotation. FARO measurements, Artec Leo scans, and photographs were obtained pre- and post-rotation. Test setup, pre- and post-rotation data acquisition, and post-processing steps, times, and considerations were noted for each measurement system (Appendix Table A1 through 3). For expediency, despite the increase in setup and post-processing time, Vicon was chosen as the measurement system for the remainder of the study and other measurement techniques were not used. The inversion wheel was reconfigured, and the process was repeated with a 90° right roll.

The restraints attach to the torso and pelvis. And throughout the testing process, it became apparent that the restraints obscured the ATD pelvis, rendering most of the measurement systems ineffective at capturing the pelvic markers. Therefore, the torso became the measure of how well the occupant was restrained, making the chest and seat markers the focus of data analysis.

This space is intentionally blank.

Static restraint system assesment.

A conventional 5-PT restraint, currently fielded in AH-64 and UH-60 helicopter pilot seats (Figure 2), and PCU-56/P TH, typically used in U.S. Navy and Air Force fighter jets (Figure 4), were evaluated using the assessment method previously described to demonstrate the developed methodology. The Vicon measurement technique was used in this demonstration for brevity in comparing the displacement of the occupant for each restraint type tested.

Individual pitch and roll rotations were performed from 0° to 45°, from 0° to 90° and from 0° to 180°, turning forward for pitch and rightward for roll (Table 1). Each test was performed three times, totaling 18 tests per restraint system.

Table 1. Static Restraint Assessment Test Matrix

Direction	Position (°)	Restraint
Forward pitch	45	TH
	90	
	180	
	45	5-PT
	90	
	180	
Right roll	45	TH
	90	
	180	
	45	5-PT
	90	
	180	

While the wheel was stabilized by two researchers, the ratchet straps and safety chains were released. The 0° starting position was verified and Vicon and Synergy were confirmed ready for data collection. Then the test director:

1. Counted down to trigger,
2. Waited one count to verify Vicon and Synergy had triggered,
3. Instructed the researchers to turn the wheel to the desired position, either 45°, 90°, or 180°,
4. Instructed the researchers to hold for five counts,
5. Intstructed the researchers acquiring data to stop recording Synergy and Vicon, and
6. Instructed the researchers to secure safety chains and ratchet straps at the final position.

Development of the Restraint Release Method

The TH, currently used in other U.S. military aircraft outside of the U.S. Army, was a complex restraint system to release as it does not have a single point release capability. The construction includes four independent latches, which caused the researchers to consider which belt to release first. Moreover, the test setup was designed to represent a completely relaxed or unconscious occupant. Thus, the final position of the occupant in roll or pitch would determine the release order of the restraints. Since MIL-S-58095A (AV) does establish a testing standard for the TH, the research team decided not to move forward with its testing (DoD, 1986).

Prior to the restraint system assessment, a restraint system release test was developed using a 5-PT restraint obtained from a UH-60M helicopter seat to measure the force required to release the buckle. The MIL-S-58095A (AV) was used as the reference to create the restraint release method for the 5-PT restraint. The MIL-S-58095A (AV) specifies that the buckle on the restraint shall be a 5-PT quick release type and have an intentional release that requires at least 5 lb in the neutral position and does not exceed 50 lb with a 250 lb occupant inverted as in a crash resulting in the aircraft resting upside down (DoD, 1986).

The release was tested in the inversion wheel separately under 180° pitch and 180° roll per MIL-S-58095A (AV). Safety chains were in place, and the locks of the caster wheels were engaged and chocked with weights (Figure 3) to prevent the inversion wheel from rotating or shifting from its location while positioning the ATD. Since no 250 lb ATD was available, an HIII-50M-P ATD weighing 176 lb was used, dressed in a green suit and loosely restrained in the test seat assembly. Safety straps were secured around the ATD to prevent it from fully falling out of the test apparatus (Figure 9). The wheel was rotated to the prescribed position.

An electronic torque wrench (ETW) Model ETW-SP-200 (Checkline, Lynbrook, NY) with an in-house fabricated adaptor to interface with the rotary buckle was used to measure the release effort. To ensure all buckles were released simultaneously, the 5-PT release was turned quickly. Incomplete releases required repetition of the test. The restraint release torque was recorded. The same operator actuated the release for each test. Photographs were taken of the inverted seat and occupant prior to the restraint system release. The ATD was then removed, and the entire setup was returned to the 0° starting position.

This space is intentionally blank.

Figure 9. The ATD was further secured with yellow safety straps to prevent it from completely falling out of the seat assembly during restraint release. This figure demonstrates the pre-release 180° roll position.

This space is intentionally blank.

Restraint release assesment.

The 5-PT release was evaluated in pitch and roll (Table 2). Each test series was performed three times, totaling 18 tests. When releasing the 5-PT restraint, there were initial issues getting all four tangs of the buckle to release. It was determined that the speed at which the buckle was turned influenced the complete release of the buckle, wherein a slow, gradual actuation sometimes failed to release all four tangs.

Table 2. Restraint Release Assessment Test Matrix

Direction	**Position (°)**
Forward pitch	45
	90
	180
Right roll	45
	90
	180

Two one-way analyses of variance (ANOVA), one for pitch and one for roll, were computed for maximum force with the configuration of the pitch or roll as the condition of interest. Each configuration had three levels for both pitch and roll: 45°, 90°, and 180°. There was a total of three groupings for maximum force. Post-hoc analyses, such as pairwise Bonferroni adjusted tests, were evaluated for any significant result in the ANOVA. All assumptions of the ANOVA were evaluated prior to use. An alpha of $p \leq 0.05$ was considered statistically significant for all statistical analyses. Statistical analyses were implemented using R (v 4.5.1) with RStudio (v 2025.5.1.513).

This space is intentionally blank.

Results

Measurement System Evaluation

The coordinates of the center chest marker in the seat axis system were calculated. The Vicon system provided coordinates at every increment of the recording, where the first and the last time points were taken as the pre- and post-rotation values, respectively. The other techniques provided single pre- and post-rotation coordinate sets. The displacement was calculated as the post-rotation minus the pre-rotation coordinates.

When the ATD was tested while wearing the TH in the 90° forward pitch, minimal displacement of the ATD was seen in the *+x, +y,* and *+z* directions (Table 3 and Figure 10) in three of the four measurement systems. Once the Vicon, FaroArm®, and Artec Leo data were analyzed, it was observed that the results measured within 0.5 in. of each other. The TEMA image tracking system demonstrated larger displacement magnitudes (3.48, 3.53, 3.52 in. compared to magnitudes of the other systems ranging from 0.04 to 0.16 in.).

Table 3. 90° Forward Pitch Chest Displacement of the ATD While Wearing the TH With Respect to the Seatback

Measurement Systems	**90° Forward Pitch Chest Displacement (in.)**			
	Run No.	***x***	***y***	***z***
Vicon	1	0.09	0.01	0.06
	2	0.09	-0.09	0.08
	3	0.08	-0.11	0.06
FaroArm®	1	0.21	-0.10	0.04
	2	0.05	0.00	0.06
	3	0.19	-0.07	0.10
Artec Leo	1	0.12	-0.07	0.15
	2	0.13	0.03	0.14
	3	0.39	0.13	-0.16
TEMA	1	-0.73	0.00	3.48
	2	-0.77	0.00	3.53
	3	-0.68	0.00	3.52

This space is intentionally blank.

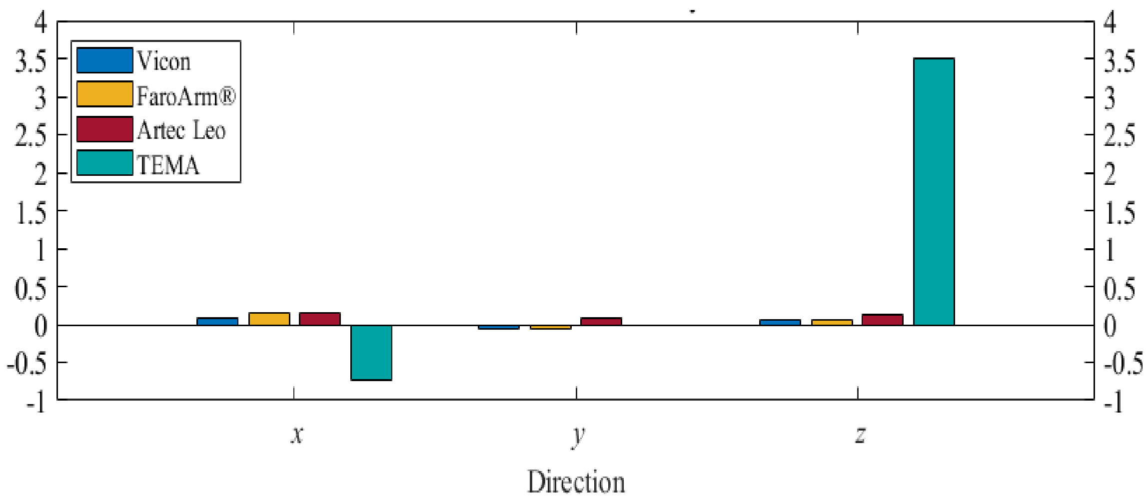

Figure 10. Chest displacement with respect to the seatback for three repetitions at 90° forward pitch rotation with the TH.

This space is intentionally blank.

While wearing the TH in the 90° rightward roll, larger displacements of the ATD were noted in the +*y* direction. Lateral displacement of the ATD for all four measurement systems was calculated to be between 3 and 6 in. Table 4 and Figure 11 show that all four measurement systems indicate that the ATD displaced primarily laterally as expected.

Table 4. 90° Right Roll Chest Displacement of the ATD While Wearing the TH With Respect to the Seatback

Measurement System	**Run No.**	**90° Right Roll Chest Displacement (in.)**		
		x	***y***	***z***
Vicon	1	0.05	-3.73	0.18
	2	0.07	-2.86	0.15
	3	0.05	-2.94	0.06
FaroArm®	1	0.12	-4.41	0.28
	2	-0.06	-3.38	0.28
	3	0.06	-3.17	0.15
Artec Leo	1	0.11	-4.27	0.19
	2	0.00	-3.49	0.06
	3	0.00	-3.00	0.09
TEMA	1	0.00	-4.01	-0.40
	2	0.00	-5.64	2.55
	3	0.00	-5.43	2.58

This space is intentionally blank.

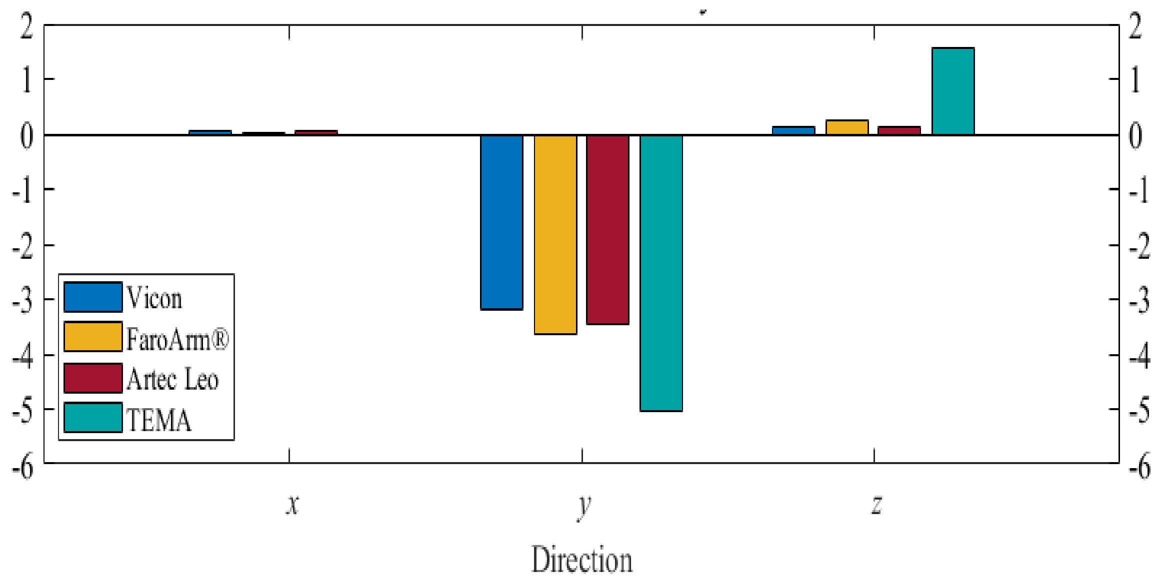

Figure 11. Chest displacement with respect to the seatback for three repetitions at 90-degree rightward roll with the TH.

This space is intentionally blank.

Static Restraint System Assessment

In order to evaluate the static restraint assessment method's ability to compare different restraints, it was used to test both a TH and a 5-PT restraint. Vicon was previously chosen as the sole measurement system for this portion of the study. The chest displacement data recorded with Vicon for the three trials of each configuration are listed in Table 5. During forward pitch, the 5-PT restraint and TH showed larger chest displacements in the +*x*- direction than in the *y*- and *z*- directions. During the right roll, both restraint systems showed higher displacements in the +*y*- direction than in the *x*- and *z*- directions. The differences in displacement between the TH and 5-PT restraint systems, which were calculated by subtracting the 5-PT means from TH means, are shown in Table 6. The static restraint assessment method was able to detect the differences between the two restraint systems, even though the differences were relatively small.

Table 5. Mean Chest Displacement With Respect to the Seatback, Recorded With Vicon

Configuration			**Mean Chest Displacement (in.)**		
Direction	**Position (°)**	**Restraint**	***x***	***y***	***z***
Forward pitch	45	TH	-0.07	0.10	-0.15
	90		0.09	-0.06	0.07
	180		0.01	0.14	1.30
	45	5-PT	0.11	0.05	-0.07
	90		0.21	-0.06	0.02
	180		-0.08	-0.46	0.65
Right roll	45	TH	-0.03	-2.37	0.02
	90		0.06	-3.17	0.13
	180		0.03	-1.82	0.85
	45	5-PT	-0.10	-1.61	0.00
	90		-0.12	-2.32	0.09
	180		-0.09	-1.32	0.74

Table 6. Difference in Mean Chest Displacement Between the 5-PT Restraint and TH

Configuration		**Difference in Mean Chest Displacement (in.)**		
Direction	**Position (°)**	***x***	***y***	***z***
Forward pitch	45	-0.18	0.05	-0.08
	90	-0.12	0.00	0.05
	180	0.09	0.60	0.65
Right roll	45	0.07	-0.76	0.02
	90	0.18	-0.85	0.04
	180	0.12	-0.50	0.11

Restraint System Release Assessment

The average torques required to release the rotary buckle for the three trials are listed in Table 7. The restraint release loads for the 5-PT restraint tested in the three pitch and three roll positions are shown in Appendix Table A4 and A5, respectively. The loads were recorded even when the restraint was not completely released as noted in the tables. The summary of these tables is displayed in Table 7.

Table 7. 5-PT Restraint Release Load Summary

Maximum Torque (in-lb)	Configuration					
	Forward Pitch			Right Roll		
	45°	**90°**	**180°**	**45°**	**90°**	**180°**
Mean	13.4	10.6	14.5	21.2	12.2	19.5
Standard deviation	4.6	2.0	4.2	5.4	3.8	6.8

The restraint release loads were higher in the right roll configuration compared to those in the pitch configuration for all runs. Even though there was a difference between the restraint release loads for the pitch and roll configurations, the 90° position for roll and pitch resulted in loads within 2 lb of each other.

This space is intentionally blank.

Assumptions of ANOVA were sufficiently met (normal residuals, homogeneity of variances, and no extreme outliers). There were no statistically significant differences in the maximum release force due to configuration for either pitch or roll (Figures 12 and 13).

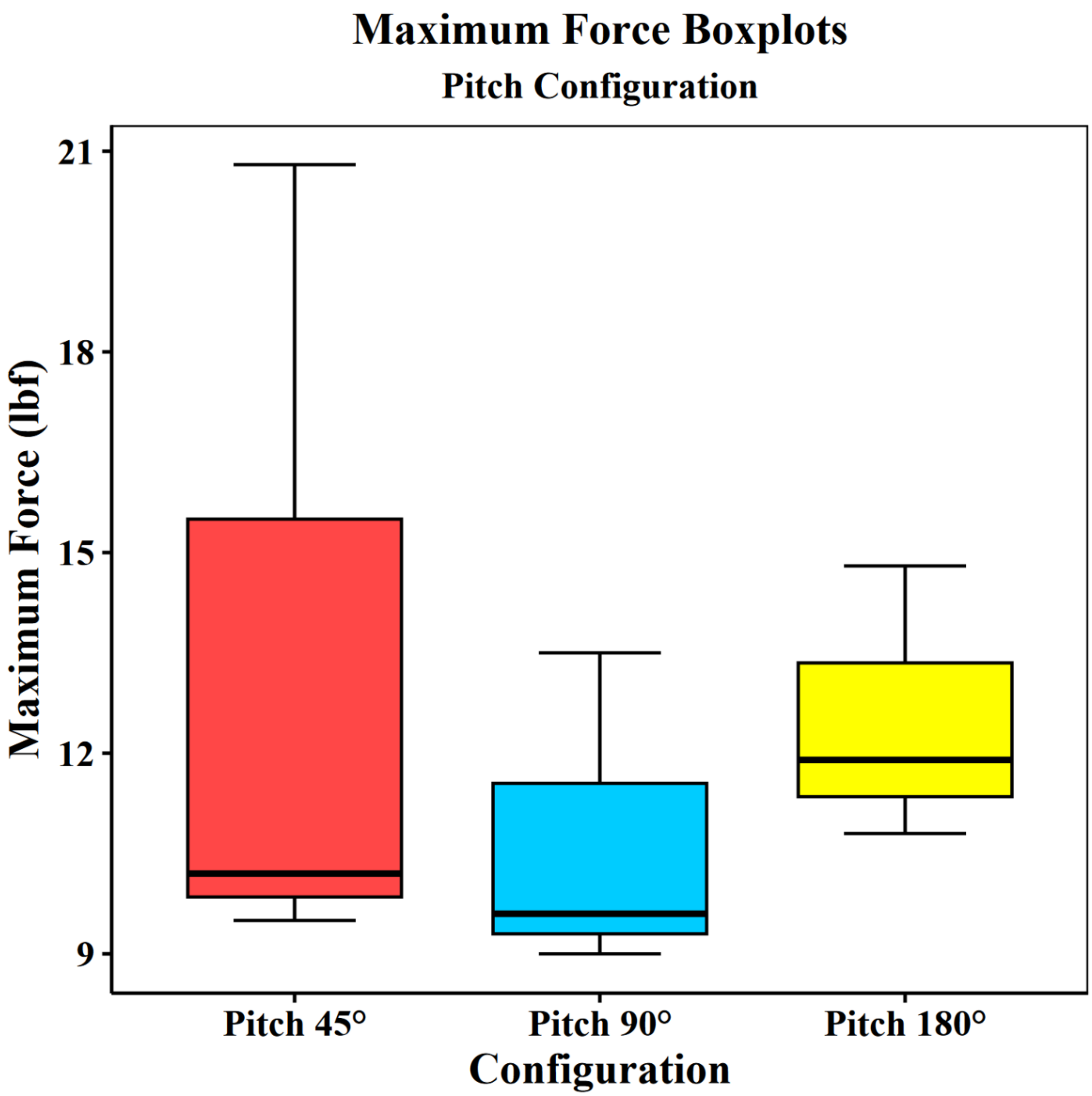

Figure 12. Boxplot results for maximum force of the restraint release mechanism for the pitch configuration at 45°, 90°, and 180° using the conventional 5-PT restraint system.

This space is intentionally blank.

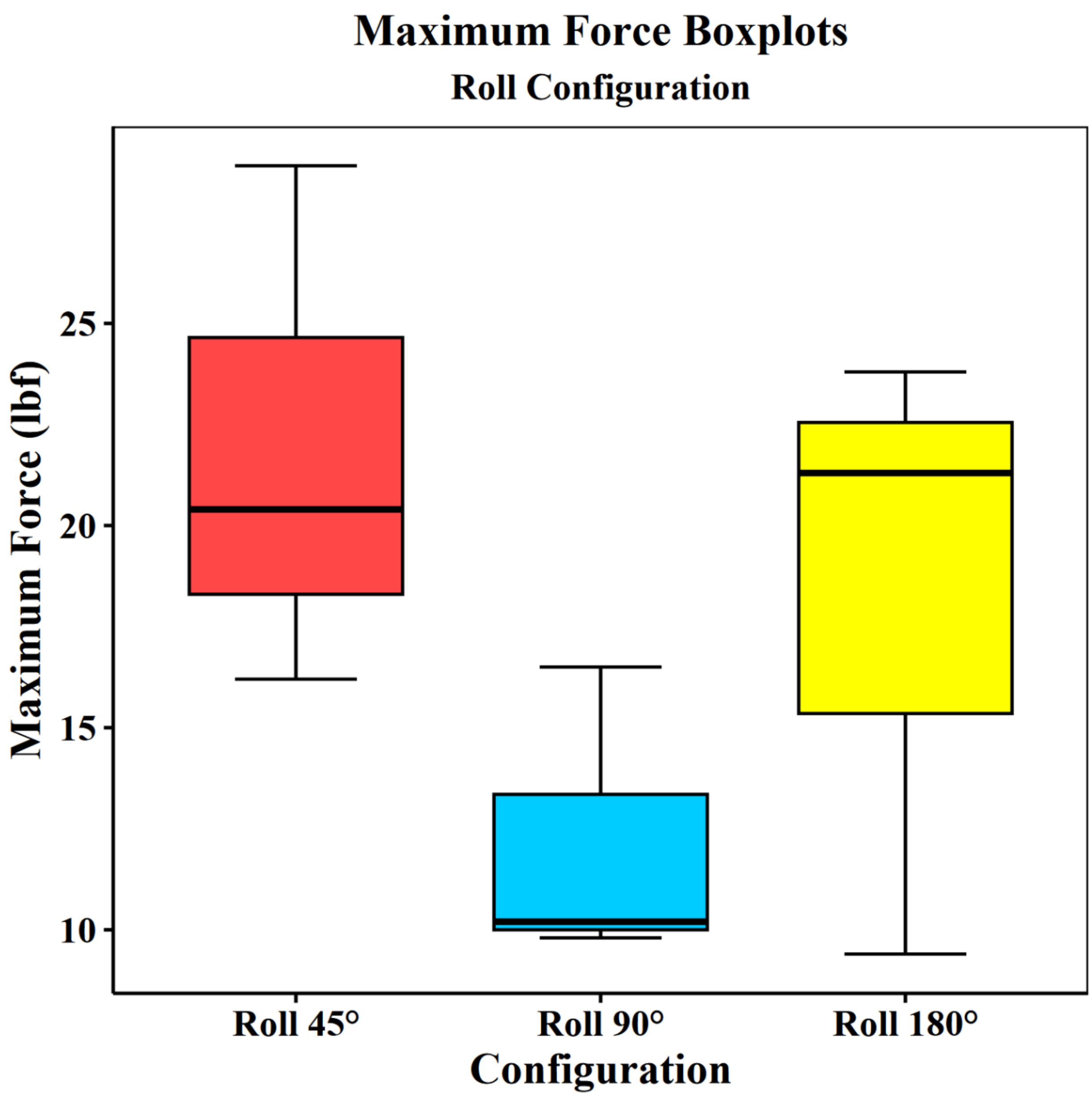

Figure 13. Boxplot results for maximum force of the restraint release mechanism for the roll configuration at 45°, 90°, and 180° using the conventional 5-PT restraint system.

This space is intentionally blank.

Discussion

ATD Selection and Positioning

Since the HIII family of ATDs are designed for dynamic impact testing, particularly representing occupants who have tensed their muscles as they are anticipating a collision, they may not represent biofidelic flail or the motion of an unbraced or unconscious occupant as well. This is particularly true of the neck, and the reason chest displacement was selected as occupant flail rather than head displacement. All this being said, perhaps a refinement could be made by using the head markers not so much as a pure biofidelic measure, but instead as a comparative measure between restraints. The HIII-50M-P has increased articulation through the hips, providing a better fit than the molded pelvis of the FAA-HIII in the 95° seat bucket angle used in this study. Although the extremity joints in the HIII-50M-P were loosened, the overall design, especially the "tensed" neck, the lumbar spine, and the rigid thoracic spine box, prevented it from flailing in a completely relaxed biofidelic manner, which suggests a more suitable ATD may be needed to represent the human body for this application.

Defining the starting position as when the seat back was vertical may have influenced the displacement measurements as the restraints could already have been preloaded by the seat angle, which removed some of the initial flail motion. If the starting position had been defined as the seat pan being positioned horizontally, then the ATD may have been able to occupy the seat unassisted by the restraints. Then, when the seat was rotated to different angular positions, the displacement measures may have been higher. This should be taken into consideration for future refinement.

Measurement System Evaluation

All chest displacement measurement techniques used the same spherical, retroreflective markers as fiducial landmarks to determine seat axes, providing an element of similarity between the results. For instance, the FaroArm® can locate intricate features, whereas Vicon captures only the retroreflective, spherical markers. Therefore, the FaroArm® also measured coordinates of the retroreflective spheres. This analysis method was also applied to Artec Leo scans and TEMA image tracking data. So, the results in Table 6 and 7 and Figures 10 and 11 show a direct comparison of the various measurement techniques.

Table 6 and Figure 10 show that the ATD displaced in the $+x$ direction, corresponding with the rotation along the pitch axis, across all measurement systems. Compared to the Vicon, FaroArm®, and Artec Leo measurement systems, the TEMA image tracking system yielded the largest displacement results in the $+x$- and $+z$- directions. Table 7 and Figure 11 show that the ATD displaced in the $+y$ direction, corresponding with the rotation along the roll axis, with all four measurement systems. Again, the analysis with TEMA resulted in larger displacement values in the $+y$- and $+z$- directions when compared to the other three measurement systems. This difference was attributed to how the images were captured for analysis with TEMA, which required more user input and additional measurements such as camera distance to the ATD, and its limitation to 2D, whereas all other systems captured in 3D.

Vicon and TEMA.

One of the challenges that the research team faced when using either the Vicon system or the TEMA camera images was that some of the markers became hidden once the test fixture was rotated. This could be improved by adding rigid extensions to the markers that do not otherwise interfere with the test. Additionally, perhaps rigidly mounting small cameras—such as Vicon or GoPro—to the inside of the inversion wheel and processing those images with Vicon or TEMA might be considered. Specific to the Vicon system, marker drop out was especially common for the pelvis, which could be mitigated by adding more cameras and placing them strategically to increase the number of cameras viewing the pelvis markers, as well as the extension mentioned above.

This methodology did not initially include TEMA tracking; however, it was added to provide a less hardware-intensive option compared to Vicon. More rigor and ground-up design considerations such as collecting the azimuth and more out-of-plane distances to relevant points, could have improved the TEMA results. However, even without these considerations, the team was able to produce viable results with TEMA as a measurement system. Lastly, using TEMA 3D instead of 2D to gain the out-of-plane motion from various camera views would be even more advantageous.

FaroArm® CMM.

Another obstacle encountered involved the USAARL inversion wheel fixture. The FaroArm® tripod needed to be partially inside of the framework of the wheel during measurements, decreasing the already small workable area. The FaroArm® operator must stand inside the wheel to collect measurement points, adding more interferences within the inversion wheel footprint (Figure 14). This was exacerbated when the wheel was rotated. For example, with the chair in a 90-degree pitch or roll, many points were obscured by the test fixture and required the FaroArm® operator to assume contorted postures while taking measurements. These actions could lead to increased potential for user error, risk of injury to the operator, and fixture, surrogate, or FaroArm® disturbance.

This space is intentionally blank.

Figure 14. The FaroArm® Quantum Max had to be positioned inside of the inversion wheel to complete measurements. Here, the test fixture is in the 90-degree roll configuration.

Additionally, the portable FaroArm® was attached to a tripod, allowing portability. With the difficulty in collecting points, significant manipulation of the FaroArm® is required, which may induce movement of the tripod and base and introduce measurement inaccuracies. To mitigate these complications, a fixed base should be used to position the FaroArm® and using a FaroArm® with a long reach of 50 in. or more is recommended.

Artec Leo and SolidWorks.

Complications introduced with the Artec Leo handheld scanner were more evident once the 3D models were analyzed in SolidWorks, such as incomplete rendering of the spherical markers. However, this can be mitigated by increasing the scanning time and reducing the surface reflectivity of the aluminum seat due to the bright LED array around the lens on the scanner.

Static Restraint System Assessment

The novel methodology was demonstrated with two restraint systems, a 5-PT restraint and a TH. The mean chest displacement results (Table 8) demonstrate that the TH and 5-PT restraint systems perform similarly at all positions in forward pitch and right roll, albeit this may have been influenced by setting the baseline position to be a vertical seat back verses a horizontal seat pan. Additionally, in roll, it was noted that both restraints allowed more lateral motion. This methodology provided reliable results and should be applicable to a variety of restraint designs to measure displacements and make comparisons across different restraint designs under static 1 G loading.

Restraint System Release Assessment

The 5-PT restraint release loads were well under the release limit of 50 lb set forth in MIL-S-58095A (AV) regardless of pitch/roll position. Probably due to the small sample size of three, there was no significant evidence that the inversion configuration for either the pitch or roll test influenced the maximum force needed to release all restraints. An ANOVA was used to statistically test this factor, but the results indicated the test design was underpowered.

It was noted that restraint release loads were slightly higher in the roll positions. Although the largest difference in means of the 5-PT restraint release loads was between the roll tests at 45° and 90°, it is possible that a significant difference between the roll and pitch configurations was missed due to the small sample size. To reduce the uncertainty, the sample size should be increased. Additionally, the absence of a significant difference may be due to the manual release technique. Perhaps this could be mitigated with a longer lever arm on the torque wrench.

And it is recognized that the available 176 lb ATD, used here to develop this restraint system release assessment method, should be replaced with one closer to the MIL-S-58095A (AV) specified 250 lb occupant to better characterize the release method presented herein.

Initial Risk Assessment

Restraint system.

The increased lateral chest motion of both restraint systems in roll could be indicative of increased occupant injury risk in that mode. This is especially important in side-facing seats due to the potential injury hazard of striking structures within the cabin interior and/or other occupants.

Restraint release.

The release on the 5-PT restraint failed to release all straps in some instances, which was originally thought to be the result of operator inexperience and methodology. However, the researchers concluded that the release failure was dependent on the rotational speed of the buckle mechanism. The rotary buckle release mechanism must be rotated quickly to release all straps, which may be a challenging feat if the occupant already has an upper extremity injury. An incomplete release of the restraint would pose a risk for the occupant to successfully egress from the aircraft.

This space is intentionally blank.

Conclusions

The developed methods were sufficient to assess restraint systems under static 1 G loading and egress efficacy. Although the TEMA method, as presented, could use considerable refinement, each of the measurement systems demonstrated the ability to reliably obtain the chest displacement, and as a whole, provide a variety of viable options from which to choose based on the performer's equipment and/or space availability. The developed static restraint system method can be used to assess other restraint systems. Two possible initial risks were identified, an increased risk of lateral flail associated with the 5-PT restraint and TH and the potential inability of the user to release the 5-PT restraint effectively. The initial risk assessment indicates a need for dynamic lateral testing to inform on occupant safety.

References

Barker, C. O., & Bellenkes, A. H. (1996). U.S. Naval helicopter mishaps: Cockpit egress problems. *Aviation, Space, and Environmental Medicine*, *67*(5), 480–485. https://asma.kglmeridian.com/view/journals/asem/67/5/article-p480.xml

De Lorenzo, R. A., Freid, R. L., & Villarin, A. R. (1999). Army aeromedical crash rates. *Military Medicine*, *164*(2), 116–118. https://doi.org/10.1093/milmed/164.2.116

Department of Defense. (1986). *Seat system: Crashworthy, non-ejection, aircrew, general specification for* (MIL-S-58095A [AV]). U.S. Department of Defense.

Desjardins, S. P., Zimmerman, R. E., Bolukbasi, A. O., & Merritt, N. A. (1989). *Aircraft crash survival design guide - Volume 4: Aircraft seats, restraints, litters, and cockpit/cabin delethalization* (USAAVSCOM TR 89-D-22D). Aviation Applied Technology Directorate, U.S. Army Aviation Research and Technology Activity. https://apps.dtic.mil/sti/pdfs/ADA218434.pdf

Hearon, B. F., Brinkley, J. W., Hudson, D. M., & Saylor, W. J. (1983). *Effects of negative G strap on restraint dynamics and human impact response* (AFAMRL-TR-83-083). Air Force Aerospace Medical Research Laboratory. https://apps.dtic.mil/sti/pdfs/ADA138642.pdf

Humanetics Innovative Solutions, Inc. (2017). *Harmonized hybrid III 50th male pedestrian user manual* (78051-9905-H). https://www.humaneticsgroup.com/sites/default/files/2020-11/um-h-h3-50m_ped_rev_a.pdf

Knapp, C. J., & Johnson, R. (1996). F-16 Class A mishaps in the U.S. Air Force, 1975-93. *Aviation, Space, and Environmental Medicine*, *67*(8), 777–783. https://asma.kglmeridian.com/view/journals/asem/67/8/article-p777.xml

Labun, L. C. (2014). *Rotorcraft crash mishap analysis* (RDECOM TR-09-D-45). U.S. Army Research, Development & Engineering Command. https://apps.dtic.mil/sti/tr/pdf/ADA508186.pdf

Sand, L. D. (1978). *Comparative injury patterns in U.S. Army helicopters* (AGARD-CP-255). AGARD Conference Proceedings, London, UK: Technical Editing and Reproduction Ltd. https://www.sto.nato.int/document/operational-helicopter-aviation-medicine/

Shanahan, D. F., & Shanahan M. O. (1989). Injury in U.S. Army helicopter crashes October 1979-September 1985. *The Journal of Trauma, 29*(4), 415–422. https://doi.org/10.1097/00005373-198904000-00001.

Shanahan, D. F., & Shanahan, M. O. (1989). Kinematics of U.S. Army helicopter crashes: 1979-85. *Aviation, Space, and Environmental Medicine*, *60*(2), 112–121. https://asma.kglmeridian.com/view/journals/asem/60/2/article-p112.xml

Willett, J. F., Rhodes, D., & McEntire, B. J. (2022). *Critical review of pilot seat and torso restraint systems for occupant protection in U.S. Army rotorcraft* (USAARL-TECH-FR--2022-48). U.S. Army Aeromedical Research Laboratory.

Appendix A. Additional Methodology Information

Table A1. Measurement System Steps, Time, and Considerations for Test Setup

Measurement System	Steps	Time	Considerations for Pre- and Post-Rotation Data Acquisition
Vicon	Iteratively set up marker set and capture volume (camera placement, aim, zoom, focus) for full range of motion. Repeat for each mode of rotation.	4 days	Marker set/capture volume may have to be individualized for each mode of rotation.
FaroArm®	Develop FARO file based on pre-determined points.	90 minutes (min)	May need to amend file once testing has started to accommodate unanticipated difficulties.
	Ensure all desired points are within the FaroArm® reach and reposition if needed.	5 min	Position the FaroArm® as close to the test seat assembly and surrogate as possible without disturbing the ATD positioning, making sure the FARO base remains fixed.
			If the FaroArm® cannot reach all points from outside of the footprint of the fixture, it needs to be positioned inside the wheel framework, limiting the allowable working space for the operator, which increases the chance for disturbance of the fixture, arm and/or ATD.
	Calibrate the FaroArm® at the beginning of testing.	15 min	A true uninclined surface is desired for best calibration, which may not be located on the fixture.
Artec Leo	NA	NA	NA
TEMA	Setup camera (leveling, focusing, and marking camera positions)	60 min	Cameras should not be moved once positioned.
	Take fixture and marker distance measurements for TEMA analysis		Ensure camera is focused on the main fixture and markers.
			Record distances and measurements for scaling to ensure consistent image analysis.

Table A2. Measurement System Steps, Time, and Considerations for Pre- and Post-Rotation Data Acquisition

Measurement System	Steps	Time	Considerations for Pre- and Post-Rotation Data Acquisition
Vicon	Calibrate cameras.	5 min	May need multiple attempts if the world error in Nexus is undesirable as determined by the lead investigator.
			May need to be repeated if cameras are bumped.
	Capture trial.	1 min	
	Reconstruct, label, fill gaps, and export tracks.	5 min	
FaroArm®	Acquire points needed for the definition of a chair-based coordinate system.	35 min	Same considerations as test setup.
	Set the origin and define axes as desired.		
	Begin collecting all points.		Post-rotation, the operator may potentially need to crouch, kneel, and lay on floor to collect points that have been rotated to the underside of the fixture/surrogate.
			Requires difficult manipulation of the FaroArm® to reach the farthest points. This increases the chance for disturbance of the fixture, arm, and surrogate.
	Review preliminary data.		NA
Artec Leo	Acquire scans.	25 min	Several passes are required for adequate capture. Not all surfaces (especially retroreflective ones) are conducive for scanning. Post-test chair position can reduce available working space and make scans difficult to acquire.
TEMA	Acquire the photographs, and measure the distances to occupant (post-rotation).	5 min	Caution should be taken not to shift cameras.
			Some markers may be obscured in certain configurations.
			Ensure the scaling landmark is visible in all photographs.

Table A3. Measurement System Steps, Time, and Considerations for Data Post-Processing

Measurement System	Steps	Time	Considerations for Pre- and Post-Rotation Data Acquisition
Vicon	Develop code.[*]	3-4 days	Once coded, processing of trials becomes very rapid.
	Import tracks, define chair-based axes system, transform all points to chair-based axes, calculate chest with respect to chair displacement, and output results (plots and tabulated).	NA	
FaroArm®	Export data for analysis.	5 min	Constructs and analysis tools can be written into the file and applied concurrently during testing.
			Measurements are recorded in CAM2 and comparisons can be made externally using Excel and MATLAB.
			Collected measurements can be exported as a text file.
Artec Leo	Download and save data from the scanner to a computer within the Artec software.	3-10 hours	Artec model processing takes hours and may need to be run overnight.
	Identify and export 3D coordinates.		
	Import data into SolidWorks for analysis.	4 hours	SolidWorks axes definition and alignment are quite tedious and time consuming.
TEMA	Convert the image, calibrate and track in TEMA.	30-45 mins	Initial point setup may be time consuming; once points are established, a template can be created.
			A lot of measurements are needed for accurate results.

[*] This code was used to analyze the FaroArm® and Artec Leo data and was not factored into the total time expenditure for these techniques. Additionally, if the Artec Leo is used as a standalone device, code development would be required.

Table A4. 5-PT Restraint Release Loads in the Pitch Configuration

Configuration	Run No.	Maximum Torque (in.-lb)	Notes
Pitch 45°	1	14.6	Left shoulder and lap belts did not release
	2	10.2	All belts released
	3	12.1	Right lap belt did not release
	4	9.5	All belts released
	5	20.8	All belts released
	Mean	*13.4*	
	Std. dev.	*4.6*	
Pitch 90°	1	8.9	Left shoulder and lap belts did not release
	2	10.0	Left shoulder and lap belts did not release
	3	12.6	Left shoulder and lap belts did not release
	4	13.5	All belts released
	5	9.6	All belts released
	6	9.0	All belts released
	Mean	*10.6*	
	Std. dev.	*2.0*	
Pitch 180°	1	14.8	All belts released
	2	10.8	All belts released
	3	20.3	Right lap belt did not release
	4	11.9	All belts released
	Mean	*14.5*	
	Std. dev.	*4.2*	

This space is intentionally blank.

Table A5. 5-PT Restraint Release Loads in the Roll Configuration

Configuration	Run No.	Maximum Torque (in.-lb)	Notes
Roll 45°	1	28.9	All belts released
	2	19.3	Right lap belt did not release
	3	20.4	All belts released
	4	16.2	All belts released
	Mean	*21.2*	
	Std. dev.	*5.4*	
Roll 90°	1	16.5	All belts released
	2	9.8	All belts released
	3	10.2	All belts released
	Mean	*12.2*	
	Std. dev.	*3.8*	
Roll 180°	1	23.3	Right lap belt did not release
	2	120.4*	All belts released
	3	9.4	All belts released
	4	23.8	All belts released
	5	21.3	All belts released
	Mean	*19.5*	
	Std. dev.	*6.8*	

*Even though all the belts were released, this data point was deemed an outlier due to double turning the torque wrench after release from the ATD colliding with the operator.

This space is intentionally blank.

U.S. ARMY AEROMEDICAL RESEARCH LABORATORY

FORT RUCKER, ALABAMA

Optimizing

HUMAN PROTECTION AND PERFORMANCE

since 1962

U.S. ARMY

FCC

MRDC